Journal of Sound and Vibration (1983) **90**(1), 29–49

NORMAL MODES OF THE MODERN ENGLISH CHURCH BELL

R. PERRIN AND T. CHARNLEY

Department of Physics, Loughborough University of Technology, LE11 3TU, England

AND

J. DEPONT†

Auckland Industrial Development Division, Department of Scientific and Industrial Research, P.O. Box 2225, Auckland, New Zealand

(*Received 27 September* 1982)

Experimental measurements of the frequencies and nodal patterns of all the partials of a good quality 214 kg English church bell up to about 9 kHz have been made. By matching these with the results of finite element calculations an understanding of the physical mechanisms generating the various partials has been achieved. This has made possible the production, for the first time, of a classification scheme for the partials with a firm physical basis, and has given considerable new insight into church bell design. In particular it is now clear just how crucial to the production of the bell's characteristic timbre is the thick ring near its rim.

1. INTRODUCTION

Group theoretical arguments show [1] that the nodal patterns of normal modes of bells consist of $2m$ meridians at equally spaced azimuths and n circles parallel to the rim where $n, m = 0, 1, 2, \ldots$. Modes with $m > 0$ all belong to degenerate doublets, for a bell with perfect axial symmetry, whose members have identical nodal patterns apart from the meridians of one lying mid-way between those of the other. Such a pair of modes constitute a campanologist's "partial". The absolute locations of the meridians are indeterminate because the axial symmetry makes all azimuths dynamically equivalent. For $m = 0$ the modes are singlets and each one on its own constitutes a partial. There are two distinct types of these singlets, namely pure "breathing" modes and pure "twisting" modes. This degeneracy structure of bell partials has been confirmed experimentally [2].

In a real bell there are always imperfections in geometry and metallurgy. The results of this for doublet partials are [3] to cause (1) the fixing of the absolute locations of the nodal meridians such that there is no obvious connection between those from different partials, (2) slight distortions of the nodal patterns, and (3) slight splittings between the frequencies of the doublet components.

With the notable exceptions of the work by Tyzzer [4] and by Grützmacher *et al.* [5] there has been little detailed study of church bell partials beyond the five lowest in frequency. This is probably because these five "musical" partials are the only ones deliberately tuned by English founders [6]. The characteristics of these for a good quality bell always approximate closely to those listed in Table 1. Some German founders claim

† Temporarily at Darwin College, University of Cambridge, Silver Street, Cambridge CB3 9EU, England.

0022-460X/83/170029+21 $03.00/0

TABLE 1

Characteristics of the "musical" partials of a typical good quality church bell

Name	Frequency ratio†	Nodal meridians	Nodal circles
Hum	1	4	0
Fundamental	2	4	1 (near rim)
Tierce	2·378	6	1 (in waist)
Quint	2·997	6	1 (near rim)
Nominal	4	8	1 (in waist)

† These frequency ratios are based on the requirement that the bell be well tempered. It is common practice in the literature to round up the theoretical ratios and quote those of Tierce and Quint as 2·4 and 3, respectively, and some founders tune to this.

to tune specifically as many as nine partials, while English founders say that if the first five are correct then the others fall into line automatically. Two of the present authors (R.P. and T.C.) have confirmed that this is indeed the case with some good quality English bells [6].

The fact that physically distinct modes, with very different frequencies, can have equal values of $2m$ and n but with the nodal circles located in different places has caused considerable confusion over notation in the literature. The traditional *ad hoc* method for classifying the partials has been to define families as having a given number of circles at roughly specified positions, e.g. "one circle near the rim" and to designate different members of a given family by quoting the number of nodal meridians $2m$. This scheme has never been satisfactory because of the anomalous position of the Hum, being the *only* partial with no circles. The present writers have also found problems with the classification of a number of higher partials, probably unknown to earlier workers, with a variety of numbers and positions of circles. Clearly a better understanding of the mechanisms responsible for the various modes is needed in order to replace the old *ad hoc* scheme by one with a firm physical basis.

We have taken a good quality modern English church bell and measured the frequencies and nodal patterns of all the partials up to about 9 kHz as accurately as our equipment would allow. Accurate measurements of the geometry of the bell were then made and used as the basis for a finite element calculation of the normal modes. The hope was that we would be able to match up experimental and theoretical modes and so decide on the physical nature of each experimentally found partial by studying the finite element solution for its form. Families of partials should then be identifiable on a firm physical basis. Hopefully this should also give some insight into bell design.

2. PRACTICAL ARRANGEMENT

The bell used in the investigation had a diameter 70·2 cm, height 56·6 cm and weighed 214 kg. It was one of a peal cast by Messrs John Taylor of Loughborough and destined for St Margaret's Church, Leigh-on-Sea, Essex. Its musical note was D. It was suspended from a substantial angle-iron tripod. The bell rested on four diesel engine valve springs spaced around a plate which could be rotated inside the tripod on a central support rod through the hole destined for the clapper assembly. This was very different from the usual practical situation where the bell is rigidly bolted to a massive cast-iron headstock with a mass comparable to its own. Such normal hanging would probably eliminate some of the modes found in the present study, especially those with large amplitudes in the crown.

3. THE VIBRATION SPECTRUM

The first stage in the investigation was to discover as many partials as possible. A mode will remain undetected if either the driver or the pick-up is located on a nodal meridian or circle. The bell was therefore excited acoustically by a set of four small loudspeakers driven by an oscillator (Brüel and Kjaer (B and K) Type 1022). To minimize damping, pick-up was with a capacity transducer (B and K Type MM0004) feeding a measuring amplifier (B and K Type 2606) and a slave filter (B and K Type 2020) frequency locked to the oscillator. Output was to an oscilloscope and recorder (B and K Type 2305).

The oscillator frequency was swept very slowly—increasing at about 0·1 Hz/s—over the range 290 Hz to 20 kHz, the lower limit being selected to be just below the Hum frequency found in preliminary investigations. The frequencies of peaks on the chart were noted and the whole procedure repeated to give spectra at five different pick-up points chosen so that it was unlikely that pick-up would be on nodes of any given partial in all cases. We were therefore confident that each partial of any significance would appear on at least one of the five traces. A total of 134 partials were found in the range up to 9300 Hz and attention was concentrated on these, details of which are listed in Table 2.

4. NATURES OF THE PARTIALS

The second stage in the investigation was to take each one of these partials in turn and, in addition to measuring the frequency of each component accurately, attempt to identify it in terms of degeneracy structure, number of nodal meridians, and number and positions of nodal circles. To do this magnetic drive near an antinode was used. A small disc of radiometal was fixed to the bell with Picein wax using a large soldering iron, and driven by a magnetic transducer (B and K Type MM0002) from the same oscillator as before. Detection was with two accelerometers (B and K Type 4344) each feeding into a preamplifier (B and K Type 2625) and a measuring amplifier/slave filter pair. Output was to a double-beam oscilloscope. One accelerometer was glued firmly to the bell either near the drive point, or diametrically opposite to it, and used as a phase reference. The other was held against the bell by hand. The component modes of the great majority of partials were successfully excited from at least one of two positions located on the rim and in the waist respectively. A few of the more feeble partials required driving from positions selected by successive approximation. In several cases it was necessary to drive deliberately on a nodal circle of one partial in order not to mask the patterns of the components of a weaker partial close in frequency to it.

For practical purposes it is convenient to divide partials with doublet structures into three categories depending on the amount of splitting Δf of the pair, which usually have roughly equal half-power bandwidths $\delta f_{1/2}$. The categories are (1) $\Delta f \geqslant 3\delta f_{1/2}$, (2) $\Delta f \leqslant \delta f_{1/2}$ and (3) $\delta f_{1/2} \leqslant \Delta f \leqslant 3\delta f_{1/2}$. It is important to realize that the distinction between these categories is not sharp and that a specific partial as defined by numbers of nodal meridians and circles (plus positions) may differ in the category into which it fits as one changes from one bell to another.

4.1. WELL-SEPARATED PAIRS

The first category, that of well-separated pairs, consists of partial components so well separated in frequency that they appeared as completely separate peaks in the spectrum. Such partials in fact nearly all had two meridians. The relative height of the two peaks seen depended upon the positions of both pick-up and driver. In the simplest, but

TABLE 2

Experimental details of partials for the 70 cm Taylor bell

Reference number	Frequency (Hz)	Splitting (Hz)	Nodal meridians	Nodal circle positions (cm)	Classification (proposed scheme)	Comments
1	292·72	0	4	None	RIR	Hum
2	585·92	0	4	16	$R=1$	Fundamental
3	692·94	0	6	29	RIR	Tierce
4	882·53	0·32	6	10	$R=1$	Quint
5	1172·0	0·6	8	29	RIR	Nominal
6	1199·7	0	2	13, 41, 66	$R=1$	
7	1393·8	—	0	16, 38, 54	β?	Minor 17th
8	1470·1	—	0	21	$T=1, \alpha$?	Twister
9	1472·8	0·3	8	10	$R=1$	Major 17th
10	1525·6	0	6	11, 26	$R=2$	
11	1559·8	0·6	4	10, 28	$R=2$	18th
12	1619·8	13·1	2	11	RA	
13	1764·3	3·2	10	29, 57	RIR	Superquint
14	1776·2	—	0	11, 54	$R=1$	
15	1948·9	0	8	11, 29	$R=2$	
16	2040·3	0	2	9, 26, 47, 58, 64	$R=2$	
17	2146·8	1·2	10	9, 60	$R=1$	
18	2155·9	—	0	3, 41, 59	$R=2$	
19	2441·2	4·3	12	15, 53	RIR	
20	2443	4	2	52	β	
21	2485·7	0	4	7, 21, 38, 66	$R=3$	
22	2540·3	2·7	4	8, 39, 53, 64	RA	
23	2550·4	4·6	6	8, 21, 37	$R=3$	
24	2617·8	1·5	10	9, 32, 63	$R=2$	
25	2718·1	1·5	2	37, 55	α	
26	2804·5	—	0	8, 20, 50, 55	$R=3$	
27	2832·5	3·9	8	9, 22, 37, 66, 72	$R=3$	
28	2858·5	0·3	2	4, 20, 36, 51, 56, 63, 66, 68	$R=3$	
29	2921·6	0·9	12	9	$R=1$	
30	3028·2	—	0	8, 20, 35, 42, 63	$R=4$	
31	3172·2	—	0	5, 18, 32, 54, 63	γ?	
32	3183·1	7·1	14	31, 54	RIR	
33	3233·5	8·3	4	7, 20, 30, 44	$R=4$	
34	3369·6	4·6	2	6, 19, 30, 42, 59	$R=4$	
35	3376·8	0	10	9, 24, 38, 62	$R=3$	
36	3403·5	0·5	6	8, 29, 39, 57, 62	RA	
37	3433·4	2·1	12	9, 32	$R=2$	
38	3514·7	2·6	4	8, 12, 30, 40, 54	$R=5$	
39	3607·1	3·5	6	8, 18, 30, 40, 56	$R=4$	
40	3678·5	—	0	13, 46	$T=2, \delta$?	Twister
41	3698·1	—	0	6, 17, 28, 40, 55, 64	$R=5$	
42	3797·6	2·0	14	10, 59	$R=1$	
43	3867·0	3·5	8	8, 18, 30, 41	$R=4$	
44	3934·8	19·4	2	4, 17, 29, 39, 49, 59	$R=5$	
45	3982·0	3·6	16	27	RIR	
46	4000·0	?	4	5, 18, 28, 38, 50, 66	α	
47	4126·8	1·1	12	7, 24, 36	$R=3$	a(48)
48	4130·3	3·5	4	10, 18, 26, 42, 55	β	a(47)
49	4269	0	10	6, 18, 32, 43, 56	$R=4$	
50	4291	?	14	10, 29	?	Rogue mode

TABLE 2—*continued*

Reference number	Frequency (Hz)	Splitting (Hz)	Nodal meridians	Nodal circle positions (cm)	Classification (proposed scheme)	Comments
51	4340	0	14	7, 28	$R=2$	
52	4357	3	6	6, 17, 28, 38, 50, 73	$R=5$	
53	4360	38	2	7, 17, 28, 35, 52, 64, 66	γ	
54	4401	33	8	7, 20, 30, 42, 67	RA	
55	4433·6	—	0	5, 14, 25, 35, 45, 56	$R=6$	
56	4543	4	4	4, 15, 25, 35, 44, 58	$R=6$	
57	4765·3	5·9	16	9, 48, 57	$R=1$	
58	4813·5	0	18	20, 26, 36, 40, 50, 61	RIR	a(59)
59	4837·9	24·4	2	7, 15, 26, 34, 42, 57, 64	$R=6$	a(58)
60	4860·3	0	6	7, 17, 26, 35, 44, 56	$R=6$	
61	5004	7	8	4, 16, 26, 35, 45, 59	$R=5$	
62	5005·5	3·0	14	8, 24, 36, 55	$R=3$	
63	5076·0	11·5	12	8, 18, 30, 41, 61	$R=4$	
64	5092	23	2	5, 15, 43, 54, 62	δ	a(65)
65	5185	—	0	7, 16, 23, 31, 39, 46, 56, 59	$R=7$	a(64)
66	5255	14	4	5, 14, 23, 31, 40, 49, 60	$R=7$	
67	5298	3	10	8, 24, 34, 43, 59	RA	
68	5346	4	16	7, 28	$R=2$	
69	5523	—	0	36, 45	ε?	
70	5563	7	10	7, 17, 27, 34, 43, 59	$R=5$	
71	5599	7	6	23, 32, 37, 46	α	
72	5676	2	20	23, 30, 37, 49, 50	RIR	
73	5721	?	2	5, 15, 23, 31, 38, 44	$R=7$	a(74)
74	5721	?	4	5, 15, 23, 31, 38, 44	γ	a(73)
75	5769	0	8	5, 16, 27, 32, 40, 49, 64	$R=6$	
76	5839	47	2	6, 14, 21, 29, 38, 43, 52, 64	ε	
77	5815	6	18	9, 54	$R=1$	
78	5878	1	14	8, 18, 29, 38, 59	$R=4$	
79	5888	5	6	4, 13, 23, 30, 38, 46, 58, 70	β	
80	5989	8	4	6, 15, 24, 32, 37, 48, 60	?	Rogue mode
81	6006	4	16	8, 22, 35, 58	$R=3$	
82	6070	?	6	7, 13, 22, 32, 38, 46, 57	$R=7$	
83	6105	4	12	7, 15, 25, 37, 42, 64	$R=5$	
84	6326	—	0	6, 13, 21, 29, 36, 42, 49, 61, 70	$R=8$	
85	6365	15	4	6, 14, 22, 29, 36, 41, 52, 61	$R=8$	
86	6402	8	12	7, 20, 27, 36, 44, 59	RA	
87	6416	2	18	9, 27, 54	$R=2$	
88	6520	4	8	4, 17, 24, 32, 38, 45, 52	$R=7$	
89	6559	4	22	?	RIR	
90	6657	2	10	6, 13, 24, 31, 37, 44, 57	$R=6$	
91	6777	36	2	4, 13, 21, 28, 35, 41, 48, 54, 62	$R=8$	
92	6817	28	16	8, 18, 29, 38, 59	$R=4$	
93	6850	12	4	4, 19, 41, 51, 62	δ	
94	6921	2	14	6, 15, 25, 34, 43, 61	$R=5$	
95	6933	72	20	11, 47, 58	$R=1$	
96	7085	0	18	7, 22, 33, 58	$R=3$	
97	7125	7	8	32, 37, 42, 49, 61	α	
98	7131	?	6	3, 12, 22, 28, 35, 41, 47, 57, 66	$R=8$	
99	7159	20	2	5, 15, 20, 27, 35, 40, 45, 59, 66	ζ	a(100)

TABLE 2—*continued*

Reference number	Frequency (Hz)	Splitting (Hz)	Nodal meridians	Nodal circle positions (cm)	Classification (proposed scheme)	Comments
100	7159	15	6	5, 12, 19, 27, 34, 40, 46, 58, 66	γ	a(99)
101	7329	0	12	6, 13, 22, 30, 38, 45, 57	$R=6$	
102	7377	4	14	7, 22, 29, 37, 46	RA	
103	7441	—	0	?	$R=9$	a(104)
104	7448	7	24	?	RIR	a(103)
105	7499	0	10	5, 13, 22, 30, 36, 44, 52	$R=7$	
106	7550	3	20	6, 27, 49, 56, 62	$R=2$	
107	7559	20	4	5, 13, 20, 26, 33, 39, 45, 55, 62	$R=9$	
108	7683	0	8	5, 12, 21, 27, 34, 40, 47, 56	$R=8$	
109	7812	7	16	4, 15, 26, 33, 42	$R=5$	
110	7824	5	8	5, 12, 23, 28, 35, 39, 46, 56	β	
111	7874	4	18	6, 18, 27, 36, 60	$R=4$	
112	8104	31	2	4, 11, 20, 25, 31, 36, 42, 49, 58, 65	$R=9$	a(113)
113	8112	8	22	?	$R=1$	a(112)
114	8142	3	14	5, 15, 22, 30, 38, 45, 63, 66, 70	$R=6$	
115	8207	5	6	4, 12, 21, 27, 32, 38, 45, 51, 60, 70	$R=9$	
116	8236	23	20	7, 22, 32	$R=3$	
117	8343	5	26	?	RIR	
118	8363	15	16	6, 13, 21, 25, 34, 41, 47, 60	RA	
119	8380	3	12	6, 15, 21, 27, 34, 40, 44, 49, 63	$R=7$	
120	8405	?	2	?	η	
121	8412	?	10	6, 14, 22, 27, 35, 40, 47, 59	$R=8$	
122	8521	12	4	4, 12, 20, 26, 32, 39, 45, 63	ε	
123	8573	6	10	6, 17, 22, 28, 34, 40, 46	α	
124	8584	—	0	5, 12, 18, 24, 30, 35, 48, 54, 61, 70	$R=10$	
125	8731	2	22	5, 26, 53	$R=2$	
126	8790	35	2	5, 13, 18, 24, 30, 36, 41, 48, 56, 60, 69	θ	
127	8812	5	18	4, 16, 24, 32, 44	$R=5$	
128	8892	?	4	1, 10, 18, 25, 29, 35, 41, 47, 52, 62, 73	$R=10$	
129	8974	6	8	5, 13, 20, 25, 31, 38, 45, 49, 58	$R=9$	
130	8981	4	20	?	$R=4$	
131	9034	5	16	6, 15, 23, 30, 37, 42	$R=6$	
132	9153	2	6	6, 16, 25, 30, 36, 41, 51, 58, 66	ε	
133	9254	5	28	?	RIR	
134	9285	1	14	4, 12, 22, 27, 34, 41, 46	$R=7$	

unlikely, case where the driver was exactly at a nodal meridian of one component, and therefore approximately at an antinodal meridian of the other, movement of the mobile pick-up around the bell showed the nodal meridians of the second of these components as lines of zero amplitude with a phase change of π across them. Selecting a point

mid-way between such a pair of nodal meridians and moving up and down the bell with the mobile pick-up gave similar changes at the nodal circles. With the driver in such a position it was, obviously, very difficult to produce much response from the other component. However, the pattern for this component could be obtained by retuning to its frequency and moving the driver, with a corresponding change of reference position, to a nodal meridian of the component already investigated. It was found, as predicted by group theoretical arguments, that the nodal circles of both components always lay at the same height on the bell, while the nodal meridians of one component always lay approximately mid-way between those of the other.

In cases where the initial position of the driver proved not to be at a nodal meridian for either component the located nodal positions were no longer zero-amplitude points but rather gave amplitude minima. Once the locations of these were found it was a simple matter to place the driver at an optimum position and proceed as before.

Singlet partials, i.e., those with zero meridians, could, obviously, be treated like one component of a well-separated pair.

4.2. DEGENERATE PAIRS

The second category can be called "degenerate pairs". When the frequencies of the doublet components differed by less than about the half-power bandwidth of either member, a single peak appeared in the spectrum regardless of the positions of driver and pick-up. For *any* driver position a nodal pattern was found which had an antinode at that position. The nodal positions of both meridians and circles were well defined but the entire pattern moved around the bell with the driver position as it was changed. This is precisely what is to be expected in the case of true degeneracy, where the relative positions of the nodal patterns of the components are fixed but their absolute locations are indeterminate until some external agency, in the present case the driver, is introduced. For the bell used in the present study the Hum provided a particularly striking example of a truly degenerate pair.

4.3. INTERMEDIATE CASE

The vast majority of partials in the present study fell into an intermediate (third) category which can be defined as having differences between component frequencies of between roughly 1 and 3 half-power bandwidths. Two close peaks separated by a shallow dip appeared in the spectrum except in the unlikely event of the driver being placed exactly on a nodal meridian of one of the pair. In this case only the other member could be "tuned in" and behaviour was then exactly as in the well-separated case.

If the driver happened to be placed midway between an antinodal meridian of one component and an antinodal meridian of the other then tuning showed two equal peaks with a minimum midway between them, i.e., an "equal-amplitude point" of the type previously described by the authors in reference [7]. When driven at this mid-frequency both components were excited equally but with a phase difference of $\pi/2$ between them. Thus as the pick-up was moved around the bell at a fixed distance from the rim the appearance was that of a travelling wave, i.e., a constant amplitude with phase changing at a constant rate per unit distance. The number of meridians attributed to the partial was determined by counting the number of times that the phase relative to the reference was either 0 or π as the pick-up was moved around the bell. Nodal circles were located as before.

In general the driver did not happen to be at either a nodal meridian or an "equal amplitude point" so that one peak of the pair was stronger than the other. Tuning to the stronger peak and moving the pick-up around the bell then showed a constant rate

of phase change as before but this time with a series of maxima and non-zero minima rather than a constant amplitude. The number of nodal meridians, but not their locations, was again most readily determined by counting the 0 and π phase positions. When meridian locations were required the position of the driver had to be altered to make the minima zero.

4.4. NODAL CIRCLES

By making measurements going around a suitable antinodal circle it was always possible to obtain an unambiguous value for the number of nodal meridians as described above. In principle it should have been a simple matter to locate and count nodal circles by moving the pick-up along an antinodal meridian. In practice this was true for most partials below the "shoulder" of the bell. However, the amplitude near the top of the bell was so small for many partials that it was often impossible to determine whether nodal circles existed there or not. Another problem was that, when circle numbers became large, they tended to appear in pairs close together. If these were separated by less than the order of size of the detecting accelerometer then it obviously became very easy to miss both of them during a meridian-wise sweep. This meant that for numerous partials the total number of experimentally found nodal circles could not be used with any confidence as a descriptive parameter and was therefore of only limited value in seeking a classification scheme. Nevertheless, the *positions* of those circles which could be observed proved to be of great value for the latter purpose.

4.5. ACCIDENTAL DEGENERACY

To the group theorist accidental degeneracy in the context of vibrations means degeneracy between modes which is not due to the symmetries of the system. In the case of a bell it would mean degeneracy between different partials, i.e., over and above those from the components of the partials. Although one might intuitively expect that such degeneracies would be rare in a bell a number were found in the present study and usually manifested themselves by a mode appearing to have different numbers of nodal meridians at say the top and bottom of the bell with a region of total confusion in the waist. In some cases this led to ambiguities over which nodal circles belonged to which partial.

4.6. EXPERIMENTAL RESULTS

Details of the experimental results are given in Table 2. The numbers of meridians quoted are accurate although, for reasons already explained, care was needed in interpreting cases with accidental degeneracy. These are emphasized in the table by comments of the type "$a(x)$" where x is the reference number of a partial with one or both of whose components the given partial exhibits accidental degeneracy. The frequencies quoted are accurate to ± 1 in the last digit. In those cases with $m > 0$, where the partials are known to be doublets for group theoretical reasons, the frequencies of both components were measured whenever this was possible. In these cases the frequency quoted is the higher of the two and the frequency difference Δf is listed.

The positions of nodal circles are quoted in the table as the distance in cm upwards from the rim along the outer bell surface at a fixed azimuth. It is difficult to estimate errors on these values because there was not only the error in detecting the phase-flip position along a given azimuth to be considered but also, due to pattern distortion, the fact that the location of a given circle for a given partial component varied somewhat as one moved circumferentially around the bell. The values quoted are averages with this variation taken into account and also, in the cases with $m > 0$, with allowance made

for any small variations between the two partial components. A realistic estimate for the error on a typical circle position would be about ± 2 cm. For comparison with results for other bells it would be desirable to convert these locations into, say, fractions of the distance from rim to shoulder. This can easily be done given that this distance was 54 cm for our Taylor bell.

5. THE FINITE ELEMENT APPROACH

In the finite element method one considers a structure of complex shape as being made up of elements of simpler shape. Expressions for the dynamic behaviour of each element are obtained, and enforcing displacement continuity across the element boundaries results in an expression for the behaviour of the whole structure observed at certain sampling points.† From this expression one obtains an eigenvalue equation for the natural frequencies which is then simplified to a manageable size by a technique known as "eigenvalue economisation". By selecting the q most suitable sampling points one can expect the first $\frac{1}{3}q$ normal modes to be reliably and accurately calculated.

Thanks to the axial symmetry of the bell one can anticipate the degeneracy structure of the normal modes, restrict attention to one member of each pair and take its amplitude to be of the form

$$\mathbf{u}(r, \theta, z') = a_x(r, z') \cos m\theta\, \hat{\mathbf{i}} + a_y(r, z') \cos m\theta\, \hat{\mathbf{j}} + a_z(r, z') \sin m\theta\, \hat{\mathbf{k}}, \tag{1}$$

where (r, θ, z') are cylindrical polar co-ordinates, with the symmetry axis of the bell as z'-axis. The unit vectors $(\hat{\mathbf{i}}, \hat{\mathbf{j}}, \hat{\mathbf{k}})$ are a right-handed orthogonal Cartesian set with $\hat{\mathbf{i}}$ lying along the symmetry axis in the sense from rim to crown and $\hat{\mathbf{j}}$ normal to this axis in some fixed reference plane. Because the axial symmetry enables one to fix the θ variation of the amplitude one is able, for finite element purposes, to model the bell as a two-dimensional structure in this reference plane. Once the geometry of the Taylor bell had been measured it was found that the set of quadrilateral elements shown in Figure 1 was appropriate. The amplitude of the other member of each degenerate pair is also given by equation (1) except that the sine and cosine functions must be interchanged.

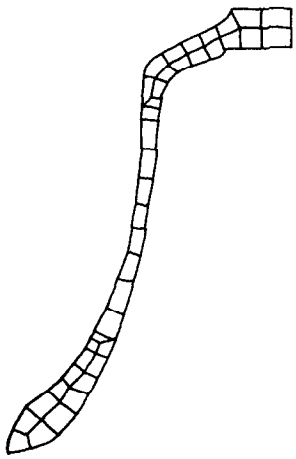

Figure 1. The finite elements used in the calculations.

† In the literature on the finite element method these points are described as "nodes". Such jargon is avoided in the present paper in order to avoid confusion with the more conventional use of the term in vibration work.

In the present work we used the finite element package known as PAFEC (Program for Automatic Finite Element Calculations) with which a separate computer run is needed for each value of m. The value of q was selected so that about the first 20 partials were expected to be calculated accurately for each m value. The values of Young's modulus, Poisson's ratio and the density for bell metal input as data were 103 GPa, 0·38 and $8{\cdot}85 \times 10^3$ kg m^{-3}, respectively. In addition to estimating the frequencies of the normal modes PAFEC was used to produce graphical displays of the amplitudes in the x–y plane. Examples are shown in Figures 2–4.

The package also produces the z-components but these could not easily be incorporated into the figures, nor would this have been particularly helpful for present purposes.

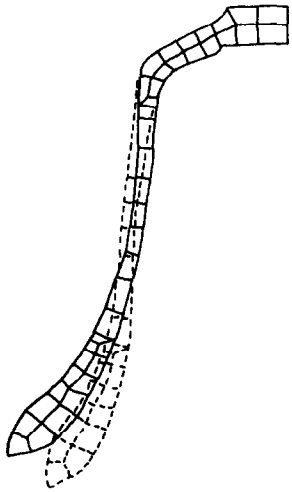

Figure 2. The six-meridian inextensional radial ring driven (RIR) mode; $2m = 6$. (Actually the Tierce.)

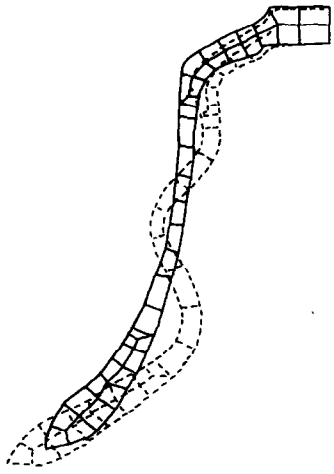

Figure 3. The six-meridian axial ring driven (RA) mode; $2m = 6$.

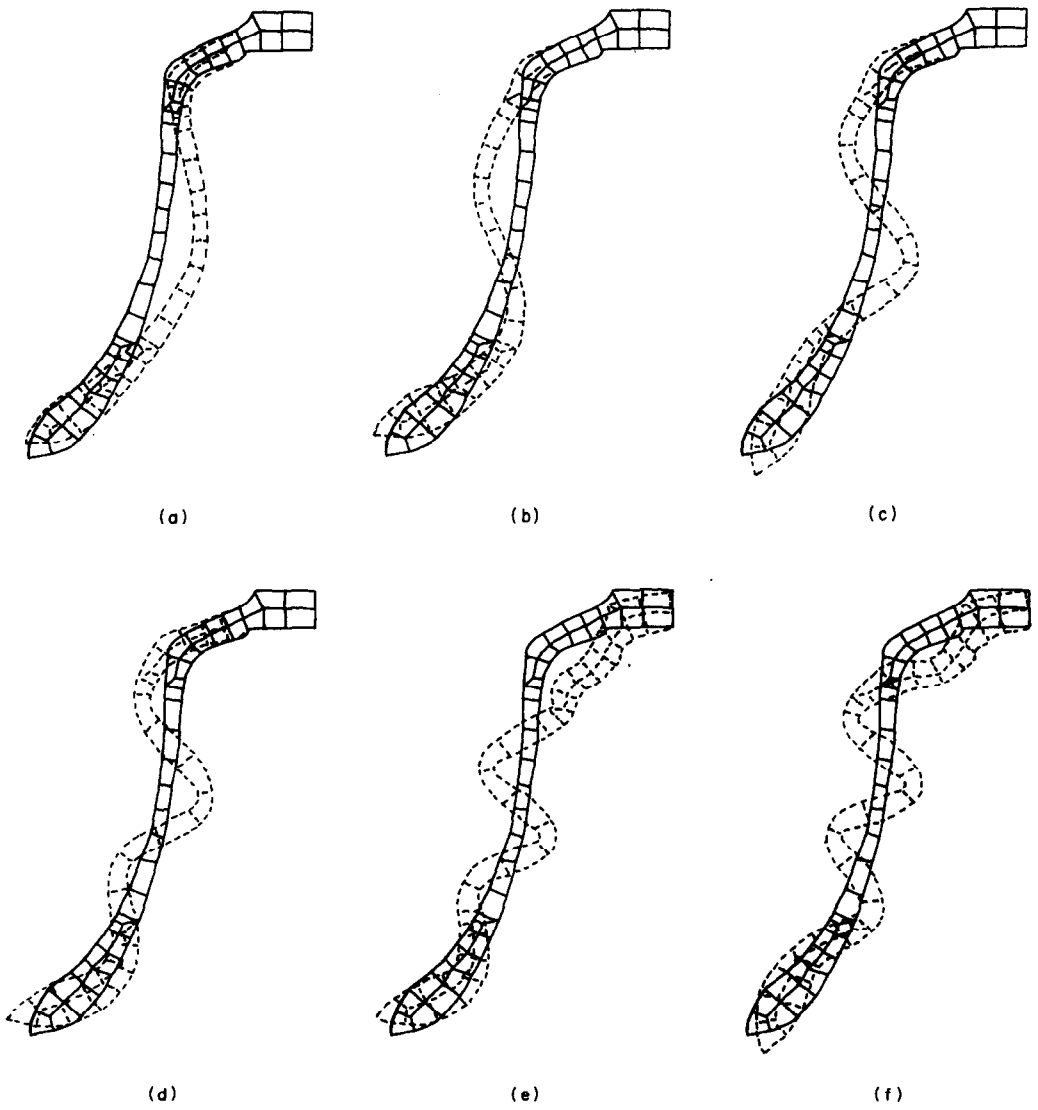

Figures 4(a)–(f). The six-meridian "shell driven" modes with $R = 1$–6. $2m = 6$; R = (a)1, (b)2, (c)3, (d)4, (e)5, (f)6.

6. COMPARISON OF EXPERIMENTAL AND FINITE ELEMENT RESULTS

Since the numbers of nodal meridans $2m$ were known reliably for both the experimental and finite element results, a comparison of these two sets of information for each value of $2m$ could be made with some confidence. Optimistically one might expect to be able to write down two lists of partials for a given $2m$ in order of increasing frequency, pair them off in sequence and so achieve agreement between both frequencies and nodal circle details. In practice things were more difficult for a number of reasons. (1) Sometimes a particular partial wrongly appeared twice in the experimental list because it had not been realized that what was present was a well-split doublet rather than single members of two doublets whose partners it had not been possible to excite. A re-identification of which modes were components of which partials was then necessary. (2) Sometimes a

partial was missing from the experimental list, although none should have been missing from the theoretical one. In many such cases it was possible to produce these missing (weak) partials experimentally in a subsidiary experiment by driving at a location and in a manner which the finite element solution indicated was likely to excite the modes. These "extra" partials have been included in Table 2. (3) Experimental nodal circle numbers and positions were often unreliable, especially above the shoulder. Although more unusual it was also sometimes the case that theoretical circle information was unreliable in regions where the amplitude became small—again usually above the shoulder. (4) The theoretical frequency predictions could be expected to be reasonably accurate early in the sequence but to become increasingly too high as one moved up it. (5) Although, after allowing for missing experimental items, the order of corresponding partials should have been the same on both lists there were some cases where two consecutive theoretical partials came out the wrong way around. It was usually nodal circle data which made it evident that this had happened, and it was always in situations where the two partials concerned were very close in frequency but of different physical types, i.e., just where one might expect rounding errors to produce such a situation.

The matching procedure was in fact carried out from $2m = 0$ up to $2m = 10$ inclusive. In order to give some idea of how it was done and how good the agreement was a listing of the frequencies for the eight-meridian case is given in Table 3. This was a particularly comprehensive example. The theoretical partial numbers 1 to 5 and 7 to 9 were well matched, in the context of the preceding comments, by the corresponding experimental items in terms of both frequency and nodal circles. The items corresponding to partial number 6 had been badly split and realization of this caused us to replace what had been listed as two separate items with missing partners in the preliminary version of Table 2 by a single badly split item. Partial numbers 10 and 13 were missing from the initial experimental list. However, a subsidiary experiment with the bell driven tangentially near the rim, as suggested by the PAFEC solution, succeeded in exciting number

TABLE 3

Comparison of finite element predictions and experimental measurements for the eight meridian partials

Mode number (PAFEC)	Frequency (Hz)		Classification (proposed scheme)
	Theory	Experiment	
1	1166	1172	RIR
2	1465	1473	$R=1$
3	1962	1949	$R=2$
4	2840	2833	$R=3$
5	3909	3867	$R=4$
6	4367	4368 4401	RA
7	5081	4997	$R=5$
8	6067	5769	$R=6$
9	6858	6516	$R=7$
10	7133	7127†	α
11	7989	7824	β
12	8201	7683	$R=8$
13	9008	—	γ
14	9782	8968	$R=9$

† Mode excited only after subsidiary experiment with suitably chosen drive arrangement.

10 which is therefore incorporated in the final version of Table 2 but has been given a dagger in Table 3. We were unable to excite number 13 even with what appeared to be a suitable driving arrangement in a subsidiary experiment. The PAFEC items 11 and 12 have come out the wrong way around, a fact which was initially ascertained by making a careful comparison of nodal circle locations, and were found to have very different physical mechanisms, as will be explained in section 7. It should be noticed that by the time PAFEC item 14 is reached the theoretical frequency has become very high compared with the experimental one, as anticipated, although the nodal circle patterns match well.

7. MODE CLASSIFICATION FOR $2m \geq 4$

The distinction between modes and partials having been drawn in section 1 one can, for purposes of producing a classification scheme, treat them as being synonymous. Also one can initially restrict discussion to modes with four meridians or more. This is because, although a scheme has been produced which is very satisfactory for $2m \geq 4$, the incorporation of modes with zero or two meridians into it has proved problematical. The reason for this is that the effective boundary conditions at the crown differ for $m = 0$ and $m = 1$ both from all cases with $m \geq 2$ and from each other. They will be more fully discussed in section 8.

The finite element solutions show that there are two broad categories of mode: (1) those primarily in-azimuthal-plane but with some out-of-plane† motion; (2) those primarily out-of-plane but with some in-plane motion. The primarily in-plane modes divide into two types which may be described as "ring driven" and "shell driven". For a given number of nodal meridians there is always one partial (provided $2m \geq 4$) which corresponds to the heavy ring at the rim of the bell going into its inextensional radial partial [8] and driving the rest of the bell. Consequently the number of nodal circles will vary depending upon the natures of the nearest modes of the rest of the bell. This family, which includes the formerly anomalous Hum as well as the Tierce and the Nominal, i.e. three of the five important musical partials, one may designate as RIR. The PAFEC diagram for the Tierce is shown in Figure 2 as a typical example. In classical ring vibration theory the inextensibility condition is written in the form $u + \partial v/\partial\theta = 0$ where $\mathbf{u} = u\hat{\mathbf{j}} + v\hat{\mathbf{k}} + w\hat{\mathbf{i}}$, which, in the notation used in equation (1), becomes $a_y = ma_z$. Thus as m increases the radial component becomes increasingly large compared with the tangential one—a feature which is particularly easy to check against the PAFEC solutions.

A second "ring driven" partial also arises for each value of $2m$ which corresponds to the rim ring going into its axial‡ mode [8]. These one may designate RA and again they do not correspond to a fixed number of nodal circles, and for the same reason. An example is shown in Figure 3. The fact that neither RIR nor RA partials correspond to a fixed number of nodal circles, so that the quantum number n is not a "good" one, explains the anomalous position of the Hum and some of the higher partials in the old *ad hoc* classification schemes.

The remaining primarily-in-plane partials, which actually form a very large majority of all partials in the region up to 9 kHz, are all essentially driven by the "bell minus rim ring" system which one may describe as the "shell". These partials are thus "shell driven" with the heavy rim ring remaining roughly at rest and supplying a nodal circle at or near the rim. For a given value of $2m$ there is a sequence of these partials which, according

† It is important to understand that the "plane" referred to here and subsequently is one, such as the reference plane introduced in section 5, which contains the symmetry axis of the bell.

‡ It is not entirely clear whether these modes are better described as "axial" or "torsional" ring driven. This point will be discussed in detail elsewhere. The important point is that they are certainly *ring* driven.

to PAFEC, have 1, 2, 3, ... nodal circles and which one may designate as forming $R = 1, 2, 3, \ldots$ families. The first six partials in the sequence for $2m = 6$ are shown in Figures 4(a)–(f). The good quantum number R is clearly related to the number n of nodal circles found experimentally in each case. However, there are frequent discrepancies between the two mainly because of extra experimental circles in the crown. This is no doubt due in large measure to the experimental problems associated with the low amplitudes in the crown region. However, it seems reasonable to suppose that these low amplitudes themselves may permit otherwise insignificant "crown driven" modes to interfere to a measurable degree with the "shell driven" ones in this region. In any event it is significant that there is seldom any disagreement concerning either the numbers or positions of nodal circles in the region below the shoulder.

From the sequence of diagrams for "shell driven" modes shown in Figures 4(a)–(f) for increasing values of R with $2m$ held fixed at 6, this being selected as a typical case, it can be seen that for low values of R the crown is essentially at rest, playing a similar role at the top of the bell to that played by the rim ring at the bottom. However, as R increases, and so the wavelength of the standing waves in the meridional direction decreases, a point is reached where the crown behaves as an integral part of the "shell" subject only to the constraint (for $2m > 2$) of a node at the very top. Further increases in R produce modes where the crown continues to participate. The value of R at which the crown "takes off" in this way increases as $2m$ increases: empirically for a given value of $2m$ the change occurs, approximately, when $R = m + 1$. The nodal circles predicted by PAFEC rise above the shoulder only after this take-off point has been passed.

Further evidence for the existence of a family relationship amongst these "shell driven" modes comes from three different ways of looking at the experimental data. (1) Plotting the positions of the nodal circles l_R against $2m$ for fixed R shows R smooth curves in each case. In Figure 5 the case of $R = 3$ is shown as a typical example. (2) Plotting l_R

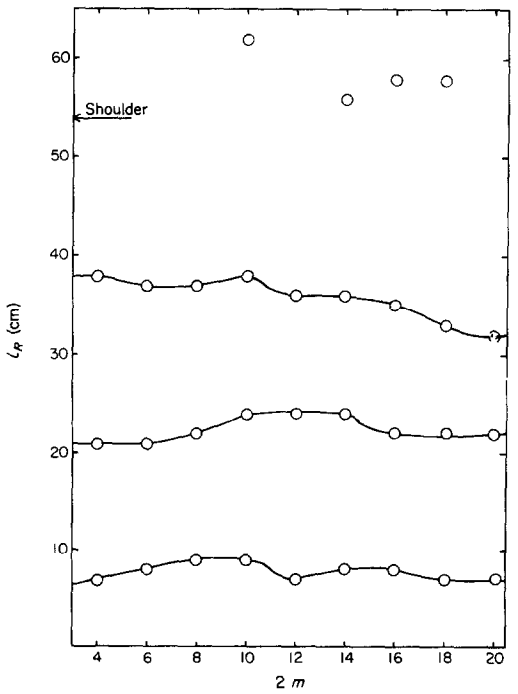

Figure 5. Graph of the ring positions against number of meridians with fixed R ($= 3$).

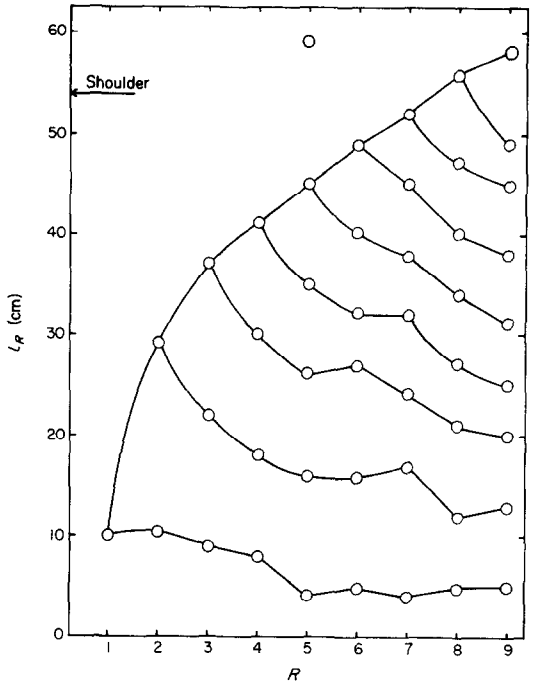

Figure 6. Graph of ring positions against R value with fixed $2m$ ($=8$).

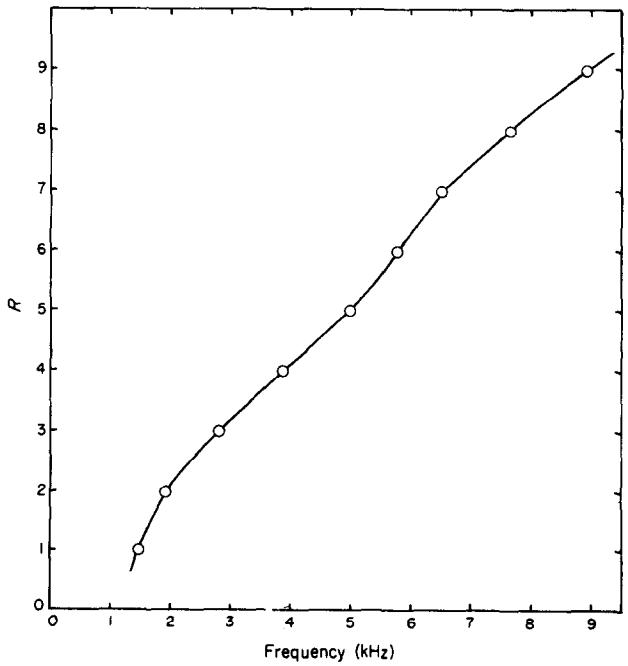

Figure 7. Graph of frequency against R value with fixed $2m$ ($=8$).

against R for fixed $2m$ shows a characteristic pattern which varies very little as $2m$ is changed. The case for $2m = 8$ is shown in Figure 6. (3) Plotting the frequency f against R for a fixed value of $2m$ yields a smooth curve, which is better than can be achieved with any other ordering or combination of modes with that value of $2m$, with a kink in the region corresponding to the crown take-off. The eight meridian case is shown in Figure 7. If one plots $\log f$ *vs.* R then the curve for fixed $2m$ is replaced, to a surprisingly good degree of approximation, by two straight lines which intersect at the point previously occupied by the kink. If the value of $2m$ is changed then a new pair of straight lines is produced. With the exception of $2m = 4$ where the situation is rather ill-defined, the position of the point of intersection is at a value of R which, approximately, increases by unity each time m increases by unity. The cases from $2m = 6$ up to $2m = 22$ inclusive are shown in Figure 8(a) while, for the sake of clarity, that for $2m = 4$ is given in Figure 8(b).

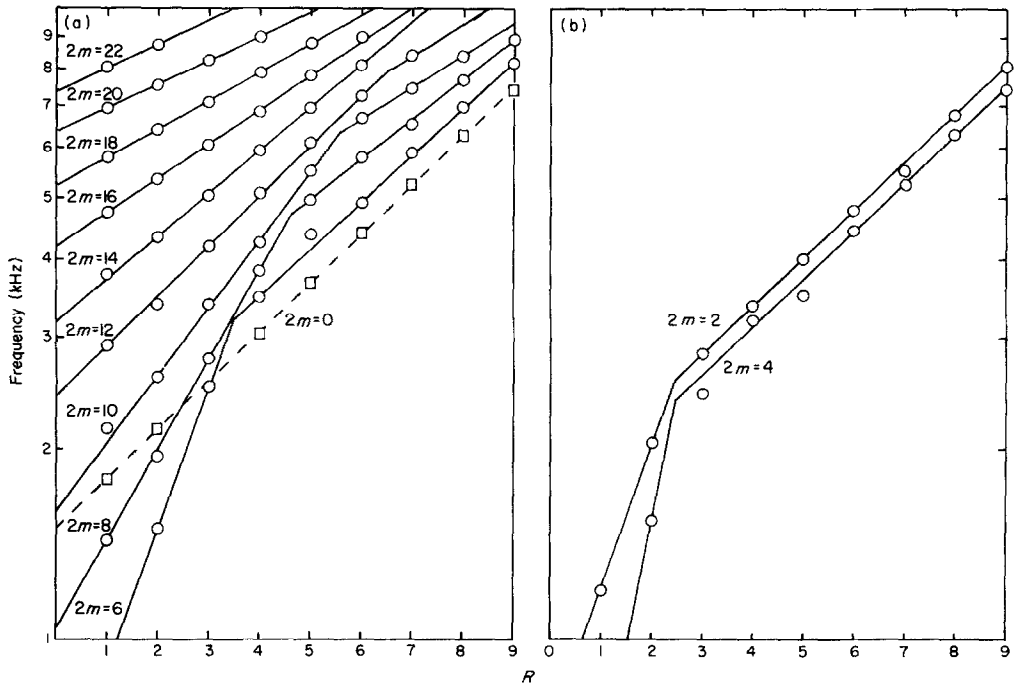

Figure 8. Graph of $\log f$ against R value with fixed $2m$: (a) $2m = 0$ and $6, 8, 10, \ldots, 22$, and (b) $2m = 2, 4$.

The modes which are primarily out-of-plane are relatively high in frequency and difficult to excite, the latter fact being responsible for a relatively high proportion of them being missing from the experimental list initially and indeed even after supplementary experiments with tangential drive. For a fixed value of $2m$ there is a sequence of these modes having an increasing number of nodal circles for out-of-plane motion. One may designate these as $\alpha, \beta, \gamma, \ldots$. The first of these is due to the heavy rim ring going into its extensional radial mode [8] and driving the shell with it, so one may give this family the alternative designation RER. The others seem to be due to various other ring sections of the bell going into their extensional radial modes in a similar way but the situation is extremely complicated. The modes were allocated to the various families mainly by examination of the out-of-plane part of the PAFEC solutions and by requiring smooth interpolation curves in the frequency against meridian number diagram to be

discussed below. Since these modes are of little acoustical importance we shall not pursue the matter in detail here. In Figure 9 the PAFEC diagram for the δ mode for $2m = 6$ is shown as a typical example but clearly, since the most important part of the motion is out-of-plane, these diagrams are not particularly helpful in these cases.

If one plots all the partials on a $2m$ versus frequency diagram then at first glance the situation is chaotic. Even when the framework of the classification scheme, which covers

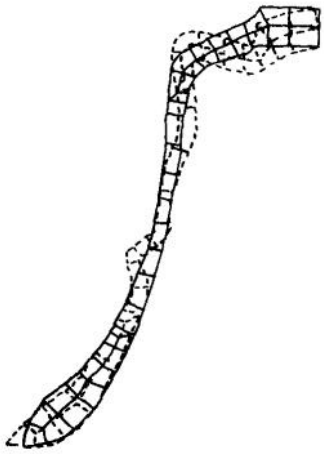

Figure 9. The six-meridian δ mode.

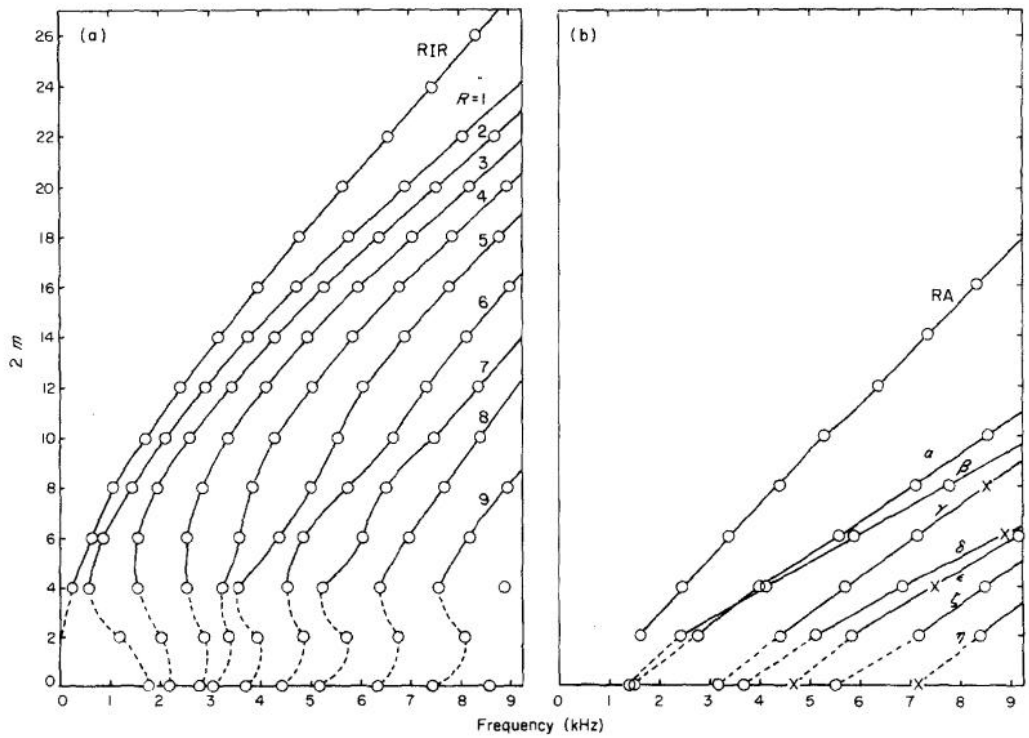

Figure 10. Graphs of meridian number against frequency for (a) the shell driven and the RIR families and (b) the families RA and $\alpha, \beta, \gamma, \ldots$.

almost every partial with $2m \geq 4$, is superimposed the situation is still very confusing. We have therefore split it up and show the various "shell driven" modes in Figure 10(a) together with the RIR family and in Figure 10(b) the primarily out-of-plane modes together with the RA family. Family relationships have been indicated in these figures by smooth interpolation curves. For completeness modes with $2m < 4$ have also been incorporated: their classification is discussed in the following section. A number of primarily out-of-plane modes were "missing", i.e., predicted by PAFEC but not detected experimentally even after subsidiary experiments. These have been incorporated into Figure 10(b), with their status clearly indicated by the use of crosses rather than circles, using their predicted frequencies. Their presence is required in order to make sense of the low population γ, δ and ε families. The approximately linear natures of all the family curves in Figure 10(b) is worthy of note: the significance of this will be discussed more fully in a further paper.

8. MODE CLASSIFICATION FOR $2m < 4$

For modes with two nodal meridians there again occurs a sequence of "shell driven" type with the rim ring essentially at rest, forcing the system to have a nodal circle at or near its location. However, there being no necessity for a node at the crown, the sequence has 2, 3, 4, ... nodal circles. These modes have been described in the literature as "swingers" [2]. The PAFEC diagram for the first member is shown in Figure 11(a). For "shell driven" modes with $2m \geq 4$ the node at the top of the crown was not counted for the purpose of deciding R values. Thus in the present case it seems reasonable to define the members of the sequence with 2, 3, 4, ... nodal circles as $R = 1, 2, 3, \ldots$ and this is the procedure that was used in drawing up Table 2. Although this approach is unambiguous and helpful it is not entirely clear whether these R designations place the modes into genuine physically meaningful family relationships with the corresponding modes with $2m > 2$. It is for this reason that the interpolation curves in Figure 10(a) are shown as broken below $2m = 4$. The tenuous nature of the family relationships is emphasized by the fact that, on the whole, these $2m = 2$ modes do not fit well onto the l_R *vs.* $2m$ curves for fixed R. However the pattern produced in the l_R *vs.* R at fixed $2m$ diagram is reasonably satisfactory apart from the appearance of an extra curve in the "above shoulder" region due to the changed effective boundary conditions in the crown. Also the log f *vs.* R diagram consists of two intersecting straight lines, shown in Figure 8(b), as in the cases with $2m \geq 4$.

Two-meridian modes, analogous to the primarily out-of-plane cases with $2m \geq 4$ in the sense that they can be classified readily by looking at the out-of-plane parts of the PAFEC solutions, also occur. These correspond to the two-meridian extensional radial modes of cylinders. The kind of problems encountered with the two-meridian "shell driven" modes do not arise. This is reflected in the way that the linear family curves in Figure 10(b) can be continued down to include the two meridian cases without difficulty. It is because we are convinced of the validity of our family allocations for these out-of-plane two meridian modes that these interpolation curves are shown in solid lines in Figure 10(b) unlike their counterparts in Figure 10(a). There is little doubt that this difference in status is connected with the fact that extensional ring modes with two meridians do occur, whereas inextensional ones do not. For interest the in-plane PAFEC diagram for the α mode with two meridians is shown in Figure 11(b).

Clearly there can be no RIR mode with two meridians because classical ring theory predicts zero frequency for inextensional radial modes with $2m = 0$ or 2. Indeed the interpolation curve for the RIR family extrapolates smoothly down to zero frequency

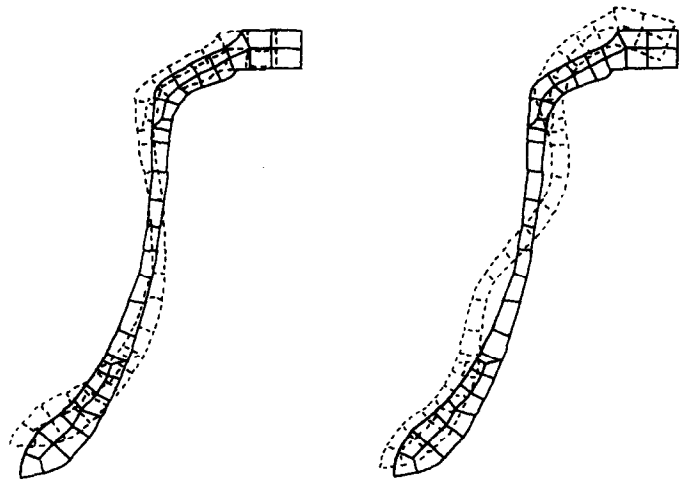

Figure 11. (a) The two-meridian shell driven mode with $R = 1$; (b) the two-meridian mode α.

at $2m = 2$ as the classical theory implies that it should. The occurrence of an RA mode with two meridians is, however, a surprise since, on the basis of classical ring theory, no such mode should occur. This is one reason why it may be more meaningful physically to regard the entire family of RA modes as torsional ring driven since a two-meridian member would then be expected.

Modes with zero meridians differ from all others in that they are not members of degenerate doublets. A consequence of this is that such modes must be either purely in-plane (e.g., "breathing" modes) or purely out-of-plane (i.e., torsional modes twisting about the bell's axis of symmetry). Also, as with the two-meridian cases, there is no necessity for a node at the top of the crown in the purely in-plane cases. The torsional modes form a sequence with 1, 2, 3, ... nodal circles for tangential motion which is designated as $T = 1, 2, 3, \ldots$ in Table 2: such modes were in fact very difficult to excite and only the first two were not "missing". There are, as expected, neither RIR nor RA modes with $2m = 0$.

From amongst the purely in-plane modes it is straightforward to select a "shell driven" set having 2, 3, 4, ... nodal circles and no node at the top of the crown which, in exactly the same way as for $2m = 2$, one can designate as $R = 1, 2, 3, \ldots$. The PAFEC diagram for the $R = 5$ case is shown in Figure 12. Like their two-meridian counterparts these "shell driven" zero-meridian modes do not fit smoothly onto the l_R *vs.* $2m$ at fixed R curves and give a l_R *vs.* R at fixed $2m$ pattern which is satisfactory apart from an extra curve in the above shoulder region. The log f *vs.* R curve is a good *single* straight line as shown in Figure 8(a): there is no crown "take-off" effect here because the crown participates fully from the start of the sequence. In Figure 10(a) the family interpolation curves can only be continued down to zero meridians in a similarly tenuous way to the two meridian cases, and for the same reasons. Nevertheless the fact that the right number of modes occur in something like reasonable places is in itself fairly impressive in view of the undoubted fundamental differences between $2m = 0, 2$ modes and the cases with $2m > 2$.

The mechanisms responsible for producing the remaining purely in-plane zero-meridian modes are complicated but seem to be due to various geometrical ring sections of the bell going into their individual breathing modes and driving the rest of the bell

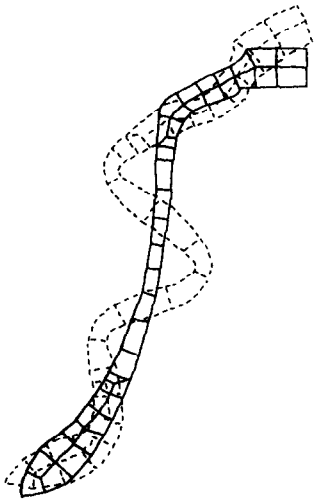

Figure 12. The zero meridian shell driven mode with $R = 5$.

in much the same way as the α, β, γ, ... families are produced for higher values of $2m$ by the extensional radial modes of such ring sections. It is perhaps therefore not too surprising to find that when these modes, plus the torsional modes and any "missing" ones, are plotted on Figure 10(b) they supply the right number in more or less the right places to fit onto extrapolations of the α, β, γ, ... family curves. We have therefore allocated the corresponding modes to these families as listed in Table 2 (with the somewhat tenuous nature of these allocations clearly indicated). However since these zero meridian modes, like their slightly less difficult two-meridian counterparts, are usually considered to be of little importance to the musical quality of the bell we shall not pursue the matter further in this article.

9. DISCUSSION

Of the five important musical partials (i.e., those specifically tuned by English founders) three are of the RIR type (the Hum, Tierce and Nominal) and the other two are of the $R = 1$ variety. Now that an understanding of the mechanisms responsible for these two families of partials has been achieved, the truly crucial role of the thick rim ring in the production of the church bell's characteristic timbre has become clear: the RIR modes are directly driven by this ring while the $R = 1$ modes, although shell driven, have their effective boundary conditions and thus their frequencies massively influenced by it. The very obvious difference in timbre between church bells and handbells is almost certainly due to the fact that no such ring is present in the latter case, rather than to any subtle differences between the remainder of their profiles (after suitable scaling). It has sometimes been suggested that the thick rim ring, being located at the clapper's strike point, serves the sole purpose of strengthening the bell there in order to avoid cracking, especially during change ringing. While the ring certainly does achieve this purpose and this could perhaps have been the original reason for its introduction there can now be little doubt that, once tested, it was retained as much for its remarkable effect upon the timbre as for any reasons of mechanical strengthening. Clearly the rim ring is the optimum clapper strike point if one wishes to maximize the relative contributions of the various RIR modes.

It is interesting that some German founders claim to tune individually not only the five musical partials of the English founders but also the musical 17th, 18th and 19th (the Superquint) relative to the Hum. The required theoretical ratios for these to be well tempered are 4·756, 5·038, 5·340 and 5·993, respectively, for the Minor 17th, Major 17th, 18th and 19th. These are to be compared with the experimental ratios for our Taylor bell of 4·762, 5·032, 5·327 and 6·016, respectively. Once the five "musical" partials have been tuned then the higher ones come out correctly "in the wash" for the Taylor bell. This implies that either the claimed teutonic thoroughness is unnecessary or else the basic shape of their bells is inferior.

The phenomenon of crown "take-off" reported in section 7 is not only extremely interesting in itself but is likely to be of importance in systems other than bells. A theoretical explanation of the empirical result that partials with $R \geqslant m$ exhibit crown participation will be reported in a subsequent paper. It seems likely that a similar effect could occur whenever the system under study contains relatively stiff and physically readily identifiable sub-systems. Within the field of percussion instruments the cymbal seems a likely candidate because of its dome-like central region. Experimental data on cymbals which seems to support this idea has been reported by Rossing [9] who, when plotting $\log f$ *vs.* $\log m$ for $n = 0$, found that his data fell on two intersecting straight lines. We would expect these to correspond to the participation and non-participation, respectively, of the central dome in the overall motion of the system. A detailed investigation of this is proceeding.

ACKNOWLEDGMENTS

The authors are indebted to Messrs John Taylor and Company, Bell Founders of Loughborough, for the loan of the bell used in this study and for access to their archives and technical expertise. In the latter respect special mention must be made of Mr M. J. Milsom and of the late Mr P. L. Taylor. Part of the work described here was undertaken while one of us (R.P.) was working as an N.R.A.C. Senior Research Fellow with the Auckland Industrial Development Division of the D.S.I.R. in New Zealand. The financial support of the N.R.A.C. during this period is gratefully acknowledged, as is the hospitality of Mr W. R. Beasley, the Director of A.I.D.D., and his staff.

REFERENCES

1. R. PERRIN and T. CHARNLEY 1973 *Journal of Sound and Vibration* **31**, 411–418. Group theory and the bell.
2. T. CHARNLEY and R. PERRIN 1975 *Journal of Sound and Vibration* **40**, 227–231. Torsional vibrations of bells.
3. R. PERRIN and T. CHARNLEY 1978 *Musical Instrument Technology* **3**, 109–117. The suppression of warble in bells.
4. F. G. TYZZER 1930 *Journal of the Franklin Institute* **210**, 55–66. Characteristics of bell vibrations.
5. M. GRÜTZMACHER, W. KALLENBACH and E. NELLESSEN 1965 *Acustica* **16**, 34–45. Acustische Untersuchungen an Kirchenglocken.
6. R. PERRIN and T. CHARNLEY 1978 *Journal of Sound and Vibration* **60**, 602–603. A note on warble in ornamented bells.
7. T. CHARNLEY and R. PERRIN 1978 *Journal of Sound and Vibration* **58**, 517–525. Studies with an eccentric bell.
8. A. E. H. LOVE 1927 *A Treatise on the Mathematical Theory of Elasticity*. New York: Dover Publications, fourth edition, 1944 re-issue. See section 293.
9. T. D. ROSSING 1982 *American Journal of Physics* **50**, 271–274. Chladni's law for vibrating plates.